

# UNIVERSITY OF BIRMINGHAM

## Research at Birmingham

### Single image super-resolution reconstruction based on genetic algorithm and regularization prior model

Li, Yangyang; Wang, Yang; Li, Yaxiao; Jiao, Licheng; Zhang, Xiangrong; Stolkin, Rustam

DOI:

[10.1016/j.ins.2016.08.049](https://doi.org/10.1016/j.ins.2016.08.049)

License:

Creative Commons: Attribution-NonCommercial-NoDerivs (CC BY-NC-ND)

*Document Version*

Peer reviewed version

*Citation for published version (Harvard):*

Li, Y, Wang, Y, Li, Y, Jiao, L, Zhang, X & Stolkin, R 2016, 'Single image super-resolution reconstruction based on genetic algorithm and regularization prior model', *Information Sciences*, vol. 372, pp. 196-207. <https://doi.org/10.1016/j.ins.2016.08.049>

[Link to publication on Research at Birmingham portal](#)

**Publisher Rights Statement:**

Checked 11/10/2016

**General rights**

Unless a licence is specified above, all rights (including copyright and moral rights) in this document are retained by the authors and/or the copyright holders. The express permission of the copyright holder must be obtained for any use of this material other than for purposes permitted by law.

- Users may freely distribute the URL that is used to identify this publication.
- Users may download and/or print one copy of the publication from the University of Birmingham research portal for the purpose of private study or non-commercial research.
- User may use extracts from the document in line with the concept of 'fair dealing' under the Copyright, Designs and Patents Act 1988 (?)
- Users may not further distribute the material nor use it for the purposes of commercial gain.

Where a licence is displayed above, please note the terms and conditions of the licence govern your use of this document.

When citing, please reference the published version.

**Take down policy**

While the University of Birmingham exercises care and attention in making items available there are rare occasions when an item has been uploaded in error or has been deemed to be commercially or otherwise sensitive.

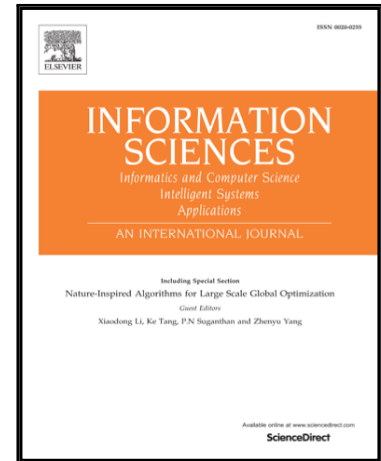
If you believe that this is the case for this document, please contact [UBIRA@lists.bham.ac.uk](mailto:UBIRA@lists.bham.ac.uk) providing details and we will remove access to the work immediately and investigate.

# Accepted Manuscript

## Single Image Super-Resolution Reconstruction Based on Genetic Algorithm and Regularization Prior Model

Yangyang Li , Yang Wang , Yaxiao Li , Licheng Jiao ,  
Xiangrong Zhang , Rustam Stolkin

PII: S0020-0255(16)30622-3  
DOI: [10.1016/j.ins.2016.08.049](https://doi.org/10.1016/j.ins.2016.08.049)  
Reference: INS 12452



To appear in: *Information Sciences*

Received date: 13 April 2015  
Revised date: 3 August 2016  
Accepted date: 15 August 2016

Please cite this article as: Yangyang Li , Yang Wang , Yaxiao Li , Licheng Jiao , Xiangrong Zhang , Rustam Stolkin , Single Image Super-Resolution Reconstruction Based on Genetic Algorithm and Regularization Prior Model, *Information Sciences* (2016), doi: [10.1016/j.ins.2016.08.049](https://doi.org/10.1016/j.ins.2016.08.049)

This is a PDF file of an unedited manuscript that has been accepted for publication. As a service to our customers we are providing this early version of the manuscript. The manuscript will undergo copyediting, typesetting, and review of the resulting proof before it is published in its final form. Please note that during the production process errors may be discovered which could affect the content, and all legal disclaimers that apply to the journal pertain.

Note to the editor – this is to confirm that I have now personally completed an extremely detailed edit of this entire paper, and that the English language is now completely correct with no errors whatsoever that I can see.

Please note:

- I am English. I was born in England; grew up in England; was educated in England at the most elite English schools and universities; and I have lived my entire life in England, except for a period of four years in USA, which is also an English speaking country.
- I completed undergraduate and masters degrees at Oxford University, England, and my PhD at University College London, England, which both demand the highest possible standards of written English.
- I have written around 100 peer-reviewed scientific papers in English.
- I have written at least 100 competitive research funding proposals in English, and lead approximately US\$10million in current research projects, for which I must provide extensive and detailed reporting to research councils (including the European Commission, various UK research councils, and UK Ministry of Defence), using English language of the highest possible standards.
- I have also published newspaper articles in English.
- I have also acted as my own patent attorney, and written several successful patents, which demand the highest possible standards of technical English writing.
- I am fully fluent in English, and have a particular reputation among my peers for being an expert in technical English writing.

If there is any part of the English writing in this paper that you still feel remains unclear, please let me know, and I will be very happy to clarify things. However, in my expert opinion, the English language writing in this paper is now of the highest academic standards.



Rustam Stolkin

Senior Birmingham Fellow in Robotics

University of Birmingham, UK

# Single Image Super-Resolution Reconstruction Based on Genetic Algorithm and Regularization Prior Model

Yangyang Li<sup>1\*</sup>, Yang Wang<sup>1</sup>, Yaxiao Li<sup>1</sup>, Licheng Jiao<sup>1</sup>, Xiangrong Zhang<sup>1</sup>, and Rustam Stolkin<sup>2</sup>

<sup>1</sup>Key Laboratory of Intelligent Perception and Image Understanding of Ministry of Education, International Research Center for Intelligent Perception and Computation, Joint International Research Laboratory of Intelligent Perception and Computation, Xidian University, Xi'an, Shaanxi Province, 710071, China

<sup>2</sup>Department of Mechanical Engineering, University of Birmingham, UK

## Abstract

Single image super-resolution (SR) reconstruction is an ill-posed inverse problem because the high-resolution (HR) image, obtained from the low-resolution (LR) image, is non-unique or unstable. In this paper, single image SR reconstruction is treated as an optimization problem, and a new single image SR method, based on a genetic algorithm and regularization prior model, is proposed. In the proposed method, the optimization problem is constructed with a regularization prior model which consists of the non-local means (NLMs) filter, total variation (TV) and adaptive sparse domain selection (ASDS) scheme for sparse representation. In order to avoid local optimization, we combine the genetic algorithm and the iterative shrinkage algorithm to deal with the regularization prior model. Compared with several other state-of-the-art algorithms, the proposed method demonstrates better performances in terms of both numerical analysis and visual effect.

*Keywords:* Single image super-resolution, genetic algorithm, regularization prior model, non-local means.

\*Corresponding author. Tel.: +86 02988202279.  
E-mail address: yyli@xidian.edu.cn (Y. Li).

## 1. Introduction

Image reconstruction plays an important role in many practical applications, such as heterogeneous image transformation [46, 47], and sketch-photo synthesis [45]. As one of the basic techniques in image reconstruction, super-resolution [21] reconstruction aims to derive a high resolution image from one or more low resolution image frames. Due to the limited capacity of imaging equipment and complex imaging environments, many situations arise where images are generated with insufficiently high-resolution (HR). Image super-resolution (SR) reconstruction technology attempts to overcome the limitations of imaging equipment and environments by recovering high frequency information which is lost during the process of low-resolution (LR) image acquisition [21]. The problem of SR reconstruction is attracting increasing interest from the imaging research community, and its solution offers significant potential for applications to video, remote sensing, medical imaging, image or video forensics, and many other fields.

Image SR reconstruction methods can broadly be divided into multi-frame image SR methods [14, 50] and single image SR methods [19, 23, 34]. With large computational complexity and storage requirements, current multi-frame SR methods can have difficulty satisfying the real-time requirements of e.g. video applications. In contrast, only using a single image as the input for the reconstruction process, enables reduced computational complexity and comparatively small data storage requirements, with the result that single image SR reconstruction methods are more widely used. Based on the two categories for SR reconstruction methods in [46], single image SR reconstruction methods can be broadly categorized into three main groups: interpolation-based methods [58, 36, 24], reconstruction-based methods [5, 37, 33] and learning-based methods [10, 6, 51, 57, 45, 15, 53, 49].

Interpolation-based SR methods use the values of adjacent pixels to estimate the values of interpolated pixels. These methods are comparatively simple and deliver real-time processing, but tend to generate HR

images with fuzzy edges, especially when the reconstruction is based on blurred or noisy LR images.

Reconstruction-based methods [25] make use of prior knowledge of reconstruction constraints. Many different kinds of priors have been incorporated into reconstruction-based methods, e.g. edge priors [43], gradient priors [42], steering kernel regression (SKR) [56, 28], non-local means (NLMs) [4, 29, 22] and total variation (TV) [30]. Alternative ideas about prior knowledge and reconstruction constraints use Markov Random Fields (MRF) to impose probabilistic constraints on pixel consistency [3, 17], and have been extended to combine these consistency constraints with predicted or expected image content [38, 39, 40]. Prior knowledge methods have proved effective at suppressing noise and preserving edges. However, these prior knowledge methods have so far demonstrated less success with respect to reconstructing plausible details [1] under large magnification.

In contrast to the above methods, learning-based methods [25] estimate the high-frequency details lost in an LR image by learning relationships between LR and HR image patch pairs from sample databases. Such methods are not generally restricted by magnification. A variety of learning-based methods for SR reconstruction have been proposed. Pioneering work by Freeman *et al.* [15] proposed an example-based image SR method. Chang *et al.* [6] established a learning model inspired by locally linear embedding (LLE). Yang *et al.* [51] used a sparse signal representation to reconstruct HR images. The method learned two dictionaries for low- and high-resolution image patches, and assumed that low- and high-resolution image patches have the same sparse representation coefficients. Yang *et al.* [52] trained the coupled dictionary by selecting patches based on standard deviation thresholding and employing a neural network model for fast sparse inference. In Wang *et al.* [45], both reconstruction fidelity and synthesis fidelity were optimized to reduce high losses on a face sketch-photo synthesis problem. Zeyde *et al.* [55] used principal component analysis (PCA) to reduce the dimension and K-SVD for dictionary training. Dong *et al.* [11]

proposed an adaptive sparse domain selection (ASDS) scheme for sparse representation, which combined data clustering and PCA to learn a set of compact sub-dictionaries. Additionally, Dong *et al* introduced autoregressive (AR) models [50] and non-local means (NLMs) to build two types of adaptive regularization (AReg) terms to improve the reconstruction quality. Recently, Dong *et al.* [10] used a deep convolutional neural network to learn mappings between low- and high-resolution images, obtaining excellent reconstruction quality.

SR can also be viewed in terms of search over a complex, noisy, high dimensional and multimodal surface. In such conditions, conventional SR methods are limited to being local in scope, by using prior information of the images to build a closed mathematical form to perform single-point search in the search space. Dong *et al.* [11] adopt the iterative shrinkage algorithm to solve the ASDS\_AReg-based sparse representation. After a sufficient number of iterations, such methods tend to converge on a local optimum, and little further progress results from additional iterations. Therefore, in this paper, we introduce genetic algorithms into the optimization process, to expand the scope of the search and help avoid convergence on local optima. GA [7, 18, 20, 35, 31] is a population-based search method that is capable of handling complex and multimodal search spaces. By increasing the diversity of solutions, GA approaches avoid local optima and offer considerable robustness for SR reconstruction problems.

In this paper, we combine genetic algorithms with ASDS\_AReg based sparse representation, and propose a single image SR reconstruction method based on a genetic algorithm (GA) and regularization prior models. Our experimental results suggest that replacing the AR with TV can improve performance. Therefore, we construct the regularization prior model by adding both NLMs and TV regularization into an ASDS-based sparse representation. We present the results of experiments, using a variety of natural images, which suggest that our method can better recover both structure and edge information, and thus improve the

quality of image reconstruction as compared with other methods from the literature.

This paper makes two main contributions:

- 1) we introduce GA into the iterative shrinkage algorithm to overcome the shortcomings of gradient-based local search algorithms;
- 2) we show how SR reconstruction can be broken down into two distinct stages: firstly, the GA is used to perform a multiple-point search to overcome local optima; secondly, the regularization prior model is then used to do a single-point search to further improve the quality of image reconstruction.

The remainder of this paper is organized as follows. Section II reviews related work. Section III describes the details of our proposed SR reconstruction method. Section IV presents the experimental results of comparing our method against other state-of-the-art methods. Section V summarizes the paper and provides concluding remarks.

## 2. Related work

In this section, we briefly review the GA, NLMs algorithm and the ASDS scheme.

### 2.1. Genetic algorithm

GA is a kind of numerical optimization method based on random search, which is inspired by the evolutionary mechanism. It was first proposed in 1975 [20]. Due to robustness against convergence on local optima, it is particularly suitable for dealing with complex and nonlinear optimization problems, such as constrained optimization problems [41] and combination optimization problems [8, 12]. The GA begins with a population initialized randomly over the search space of the optimization problem. It simulates the Darwinian evolution principle of “survival of the fittest” and generates improved approximate solutions or the optimal solution through an iterative procedure of generational evolution.

### 2.2. Nonlocal means



NLMs [29] exploit the fact that many repetitive patterns exist in natural images, and assume that a pixel can be approximated by a weighted combination of the pixels in its relevant neighborhood, i.e.:

$$\hat{X}_i = \frac{\sum_{j \in P_i} w_{ij} X_j}{\sum_{j \in P_i} w_{ij}} \quad (1)$$

where  $\hat{X}_i$  is the estimate of  $X_i$ , which denotes the  $i$ th pixel in  $X$ .  $P_i$  is the index set of pixels in its relevant neighborhood. The weight  $w_{ij}$  denotes the similarity between the neighborhood of pixel  $X_i$  and its relevant neighborhood of pixel  $X_j$  and is calculated as:

$$w_{ij} = \exp \left( - \frac{\|N_i - N_j\|_G^2}{h^2} \right) \quad (2)$$

$N_i$  and  $N_j$  represent the column vectors formed by expanding the neighborhood pixels of  $X_i$  and  $X_j$  in lexicographic ordering respectively.  $h$  is a global smoothing parameter that controls the decay of the smoothing, and  $G$  is a kernel matrix that assigns a larger weight to the pixels closed to the target pixel.

### 2.3. Adaptive sparse domain selection

The ASDS scheme, proposed by Dong *et al.* [11], learns a series of compact sub-dictionaries from example image patches, and adaptively assigns each local patch the best sub-dictionary that is most relevant to the local patch. ASDS proceeds according to two steps: learning of sub-dictionaries and adaptive selection of the sub-dictionary, which are explained in the following two subsections.

#### 2.3.1. Learning sub-dictionaries:

$M$  image patches  $S = [s_1, s_2, \dots, s_M]$  containing edge structures are selected, and are then high-pass filtered to generate an edge dataset  $S^h = [s_1^h, s_2^h, \dots, s_M^h]$ . We partition  $S^h$  into  $K$  clusters  $\{C_1, C_2, \dots, C_K\}$  using the K-means algorithm, with  $u_k$  the centroid of cluster  $C_k$ . Correspondingly, the dataset  $S$  can be clustered into  $K$  subsets  $S_k, k = 1, 2, \dots, K$ . We learn sub-dictionaries  $\Phi_k, k = 1, 2, \dots, K$ , from subsets  $S_k$  using principal component analysis (PCA) [59, 60].

#### 2.3.2. Adaptive selection of the sub-dictionary

$K$  pairs  $\{\Phi_k, \mu_k\}$  are obtained by: first, learning a dictionary  $\Phi_k$  for each subset  $S_k$ ; and then computing the centroid  $\mu_k$  of each cluster  $C_k$  associated with  $S_k$ . Next, we select the sub-dictionary for  $\hat{x}_i$  by comparing the high-pass filtered patch  $\hat{x}_i^h$  of  $\hat{x}_i$  with the centroid  $\mu_k$ :

$$k_i = \arg \min_k \|\Phi_c \hat{x}_i^h - \Phi_c \mu_k\|_2 \quad (3)$$

$\Phi_c$  represents the most significant eigenvectors from the PCA transformation matrix of  $U$ .  $U = [\mu_1, \mu_2, \dots, \mu_k]$  is the matrix containing all the centroids.

The  $k_i^{\text{th}}$  sub-dictionary  $\Phi_{k_i}$  will be selected and assigned to patch  $\hat{x}_i$ .

The whole image  $X$  can then be reconstructed by making use of information from all of the patches  $\hat{x}_i$ , written as [13]:

$$\hat{X} = \left( \sum_{i=1}^Q R_i^T R_i \right)^{-1} \sum_{i=1}^Q (R_i^T \Phi_{k_i} \alpha_i) \quad (4)$$

In [11] this is re-written for convenience as:

$$\hat{X} = \Phi \circ \alpha \hat{=} \left( \sum_{i=1}^Q R_i^T R_i \right)^{-1} \sum_{i=1}^Q (R_i^T \Phi_{k_i} \alpha_i) \quad (5)$$

where  $\Phi$  is the concatenation of all sub-dictionaries  $\{\Phi_k\}$ ,  $\alpha$  is the concatenation of all  $\alpha_i$ ,  $\alpha_i$  denotes the sparse representation coefficients of the patch  $\hat{x}_i$ ,  $R_i$  is an operator that obtains the image patch  $\hat{x}_i$  from  $\hat{x}$ , and  $Q$  is the number of patches.

### 3. Proposed SR reconstruction method

For single image SR reconstruction problems, the process of obtaining a HR image from a LR image can be generally modeled as:

$$Y = DHX + v \quad (6)$$

where  $Y$  is the LR image,  $X$  is the unknown HR image to be estimated,  $D$  is a down-sampling operator,  $H$  is a blurring operator, and  $V$  is additive noise. Therefore, the process of HR image reconstruction is an ill-posed inverse problem [2].

To make the problem well-posed, we incorporate both the non-local similarity regularization and TV regularization methods into an ASDS-AReg sparse representation:

$$\hat{\alpha} = \arg \min_{\alpha} \left\{ \|y - DH\Phi \circ \alpha\|_2^2 + \mu \cdot \|(I - W)\Phi \circ \alpha\|_2^2 + \lambda \|\Phi \circ \alpha\|_1 + \sum_{i=1}^Q \sum_{j=1}^q \gamma_{i,j} |\alpha_{i,j}| \right\} \quad (7)$$

$$\hat{X} = \Phi \circ \hat{\alpha} \hat{=} \left( \sum_{i=1}^Q R_i^T R_i \right)^{-1} \sum_{i=1}^Q (R_i^T \Phi_{k_i} \hat{\alpha}_i) \quad (8)$$

In Eq.(7),  $I$  is the identity matrix, and the first  $l_2$ -norm term is the fidelity term; the second term is the non-local similarity regularization term, and  $\mu$  is the trade-off parameter to balance the non-local similarity regularization term. The third  $l_1$ -norm term is the total variation regularization term and  $\lambda$  is the trade-off parameter to balance the total variation regularization term.  $\alpha_{i,j}$  is the coefficient associated with the  $j^{\text{th}}$  atom of  $\Phi_{k_i}$  and  $\lambda_{i,j}$  is the weight assigned to  $\alpha_{i,j}$ .  $Q$  is the number of patches and  $q$  is the number of pixels of each patch. We use the iterative shrinkage algorithm [9] to solve Eq. (7). The details of this computation process can be found in [11].

Due to blurring, down sampling and additive noise, the HR image obtained from a LR image is non-unique. Eq. (7) builds a closed mathematical form to perform single-point search in the search space by using an iterative shrinkage algorithm. In order to avoid local optima, we incorporate the GA [27] into the iterative shrinkage algorithm to solve the regularization prior model.

The detailed implementation of the SR reconstruction algorithm is presented in Table 1 and Table 2.

Table 1 Proposed image SR reconstruction algorithm.

Objective: Estimate HR image  $\hat{X}$

Inputs:

- LR image  $Y$ .
- Upscaling factor  $s$ .

Output: the final HR image  $\hat{X}$ .

Steps:

1) Initialization:

- a) Upscale  $Y$  with, using bi-cubic interpolation, by a factor of  $s$ , and obtain initial HR estimation  $X^0$ ;
- b) With the initial estimate  $X^0$ , we select the sub-dictionary  $\Phi_{k_i}$  and calculate  $W$  for the non-local weights;
- c) Preset  $\gamma, \lambda, \mu$  and the maximum iteration number, denoted by  $\text{Max\_Iter}$ ;
- d) Set  $t=0$ .

2) Iteration on  $t$  until  $t \geq \text{Max\_Iter}$  is satisfied.

- a)  $X^{(t+1/2)} = X^t + (Uy - UX^t - VX^t)$ , where  $U = (DH)^T DH$  and  $V = \mu(I - W)^T(I - W) + \lambda I$ ;
- b) Compute  $\alpha^{(t+1/2)} = [\Phi_{k_1}^T R_1 X^{(t+1/2)}, \dots, \Phi_{k_N}^T R_N X^{(t+1/2)}]$ , where  $N$  is the total number of image patches;
- c)  $\alpha_{i,j}^{(t+1)} = \text{soft}(\alpha_{i,j}^{(t+1/2)}, \tau_{i,j})$ , where  $\text{soft}(\cdot, \tau_{i,j})$  is a soft thresholding function with threshold  $\tau_{i,j}$ ;
- d) Compute  $\hat{X}^{(t+1)} = \Phi \circ \alpha_i^{(t+1)}$  using Eq.(8), which can be calculated by first reconstructing each image patch with  $\hat{X}_i = \Phi_{k_i}$  and then averaging all the reconstructed image patches;
- e) If  $\text{mod}(k, P) = 0$ , we use genetic algorithm to optimize HR estimation  $\hat{X}^{(t+1)}$  and obtain an improved solution  $X^{(t+1)}$ . The detailed implementation steps are shown in table 2;
- f) Update the matrices  $W$  using the improved estimate  $\hat{X}^t$ ;

Table 2 Details of implementation of genetic algorithm.

Input:  $\hat{X}^{(t+1)}$

Output :  $X^{(t+1)}$

Steps:

1) **Initialization:**

a) One new matrix can be constructed by replacing every  $x_{u,v}$  (the element in  $i$ th row and  $j$ th column of  $\hat{X}^{(t+1)}$ ) with  $\tilde{x}_{u,v} = P\{x_{u,v} + \Delta\}$ , where  $\Delta$  is a floating value and  $P(x)$  can be calculated as:

$$P(x) = \begin{cases} 0, & x < 0 \\ 255, & x > 255 \\ x, & \text{else} \end{cases}$$

After  $N-1$  new matrixes are generated, the initial population  $\hat{X}$  consists of the  $N-1$  new matrices and  $\hat{X}^{(t+1)}$ .

b) Fitness function:  $F_i = 1 / (E_i + \varepsilon)$ ,  $E_i = \|Y - DH \hat{X}_i\|_2^2$ ,  $i = 1, 2, \dots, N$ .  $\hat{X}_i$  is the  $i$ th of  $\hat{X}$ .

c) Set  $k=0$ .

2) **Iteration:**

Perform the following steps  $K$  times.

a) Crossover:

The crossover probability  $p_c$  of each individual is calculated as:

$$p_c = \begin{cases} p_{c1}, & f < f_{avg} \\ p_{c1} \frac{(p_{c1} - p_{c2})(f - f_{avg})}{f_{max} - f_{avg}}, & f \geq f_{avg} \end{cases}$$

Based on the crossover probabilities, two individuals  $\hat{x}_1^k$  and  $\hat{x}_2^k$  should be selected using roulette selection, and used to generate two new solutions as:

$$\begin{cases} \hat{x}_1^{k+1} = \alpha \hat{x}_1^k + (1 - \alpha) \hat{x}_2^k \\ \hat{x}_2^{k+1} = \alpha \hat{x}_2^k + (1 - \alpha) \hat{x}_1^k \end{cases}$$

where  $\alpha$  is a random number in  $[0, 1]$ .

b) Mutation:

The mutation probability  $p_m$  of each new individual is calculated as:

$$p_m = \begin{cases} p_{m1}, & f < f_{avg} \\ p_{m1} - \frac{(p_{m1} - p_{m2})(f_{max} - f)}{f_{max} - f_{avg}}, & f \geq f_{avg} \end{cases}.$$

If one random number  $r_1 \in [0,1]$  is smaller than  $p_m$ , the individual should be modified by performing the following operation:

$$\hat{X}^{k+1} = \hat{X}^k + \beta D^T H^T (Y - DH \hat{X}^k)$$

c) Selection:

With crossover and mutation,  $N$  new individuals will be generated and combined with the parental  $N$  individuals. Among the  $2*N$  individuals, the best  $N$  individuals will be selected as the parental individuals in the next generation.

In above equations,  $f_{max}$  is the maximum fitness value of the population,  $f_{avg}$  is the average fitness value of the population,  $f$  is the fitness value of the individual.

#### 4. Experimental results and analysis

To validate the effectiveness of the proposed method, we have conducted empirical experiments on a variety of natural images. We compare our proposed method against a variety of state-of-the-art methods, including SC-based [51], ASDS [11], SPM [32], ANR [44], AULF [54]. *Peak Signal to Noise Ratio* (PSNR) and *Structural Similarity* (SSIM) [16, 48] are used as objective quality measures of the SR reconstruction results. All tests are carried out using only the luminance component of color images, because human vision is most sensitive to the luminance component, and the bi-cubic interpolator is applied to the chromatic components.

##### 4.1. Experimental Settings

In our experiments, the input LR images are generated from the original HR image by a  $7 \times 7$  Gaussian kernel of standard deviation 1.6 and decimated by a factor of 3. For the noisy images, the Gaussian white noise with standard deviation of 5 is added to the LR images. In the first stage, the number of iterations is 10, population size  $N=30$ ,  $p_{c1}=0.9$ ,  $p_{c2}=0.6$ ,  $p_{m1}=0.1$ ,  $p_{m2}=0.001$ ,  $\Delta$  is random value in  $[-8, 8]$ . In the second stage, the maximum iteration time for gradient descent is set at 200 iterations; the regularization

parameters  $\mu$  and  $\lambda$  are set to 0.04 and 0.03 for the noiseless images and 0.6 and 0.45 for the noisy images, respectively. For the calculation of NLMs weight  $W$ , we set the smoothing parameter  $h$  to 10, and the patch size to  $7 \times 7$ . Neighbors are considered to be those lying within a  $13 \times 13$  neighbourhood. Four iterations are alternately performed during the aforementioned two stages.

#### 4.2. Effectiveness of introducing GA

To validate the effectiveness of introducing the GA to the iterative algorithm, we compare the SR performance on five test images. PSNR and SSIM are tabulated in Table 3 and the results suggest that the addition of the GA can improve performance.

Table 3 Performance comparison between the algorithms with and without GA.

Image	Butterfly	Hat	Leaves	bike	Comic
Without GA	27.97	31.21	27.20	24.65	24.39
	0.917	0.874	0.914	0.798	0.785
Introduced GA	28.35	31.39	27.55	24.75	24.55
	0.922	0.878	0.923	0.800	0.787

#### 4.3. Experiments on images without artificially added noise

In this subsection, we conduct experiments on 8 images to evaluate SR performance in comparison with five other state-of-the-art methods. The first four images are the same as those used in [11] and the remaining four images are chosen from the BSDS500 image database as shown in Fig. 1. The objective evaluation results of PSNR and SSIM are presented in Table 4. The proposed method performs better than all the comparison methods in terms of the averaged results of PSNR and SSIM.

Table 4 PSNR (dB) and SSIM results of eight test images for  $3\times$  magnification( $\sigma_n = 0$ ).

Test image	SC [51]	SPM [32]	ANR [44]	ASDS [11]	AULF [54]	Proposed method
Butterfly	25.15 0.853	26.74 0.897	25.50 0.862	27.34 0.905	27.94 0.912	<b>28.35</b> <b>0.922</b>
Hat	30.15 0.854	30.84 0.867	30.09 0.854	30.93 0.871	<b>31.51</b> <b>0.880</b>	<b>31.51</b> 0.879
Leaves	24.62 0.846	25.84 0.889	24.91 0.855	26.78 0.905	27.00 0.913	<b>27.55</b> <b>0.923</b>
Plants	31.94 0.885	32.83 0.904	32.26 0.895	33.47 0.910	33.72 0.909	<b>33.83</b> <b>0.922</b>
Elephants	30.72 0.786	31.35 0.806	30.94 0.798	31.18 0.803	31.61 <b>0.811</b>	<b>31.75</b> <b>0.814</b>
Woman	30.72 0.896	31.62 0.925	30.68 0.913	31.63 0.922	31.83 0.923	<b>32.33</b> <b>0.927</b>
Red flower	30.16 0.872	31.09 0.893	30.63 0.884	30.91 0.891	30.96 0.887	<b>31.21</b> <b>0.893</b>
Building	24.88 0.710	25.74 0.741	25.07 0.717	25.57 0.745	25.99 0.754	<b>26.17</b> <b>0.763</b>
average	28.54 0.830	29.50 0.865	28.76 0.851	29.72 0.869	30.07 0.873	<b>30.33</b> <b>0.880</b>

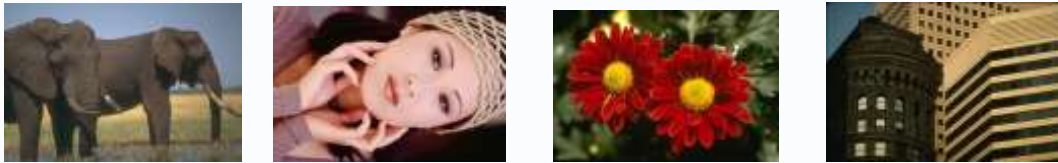
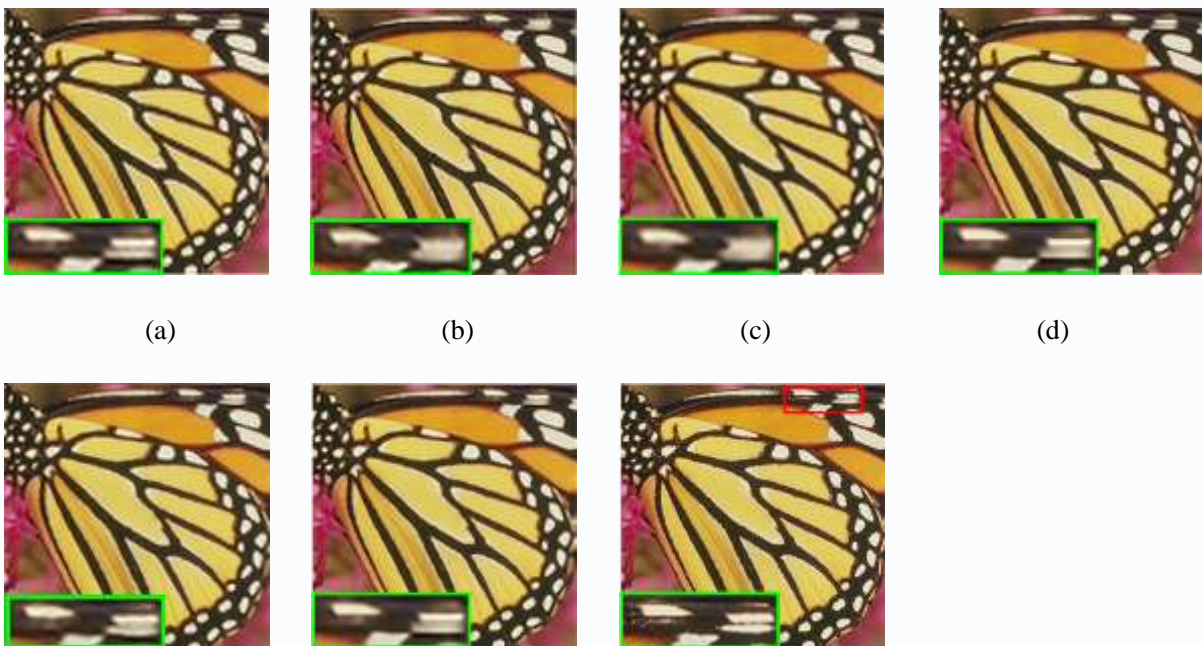


Fig.1. Test images used in Table 4. We refer to the images in Table 4 by its position in the raster scanning order.





(e) (f) (g)

Fig.2. Super-resolved images ( $3\times$ ) of Butterfly with different methods. The area in green rectangle is the  $2\times$  local magnification of red rectangle in each example. (a) Result of SC-based method. (b) Result of SPM. (c) Result of ANR. (d) Result of ASDS. (e) Result of AULF. (f) Result of proposed method. (g) The original HR image.

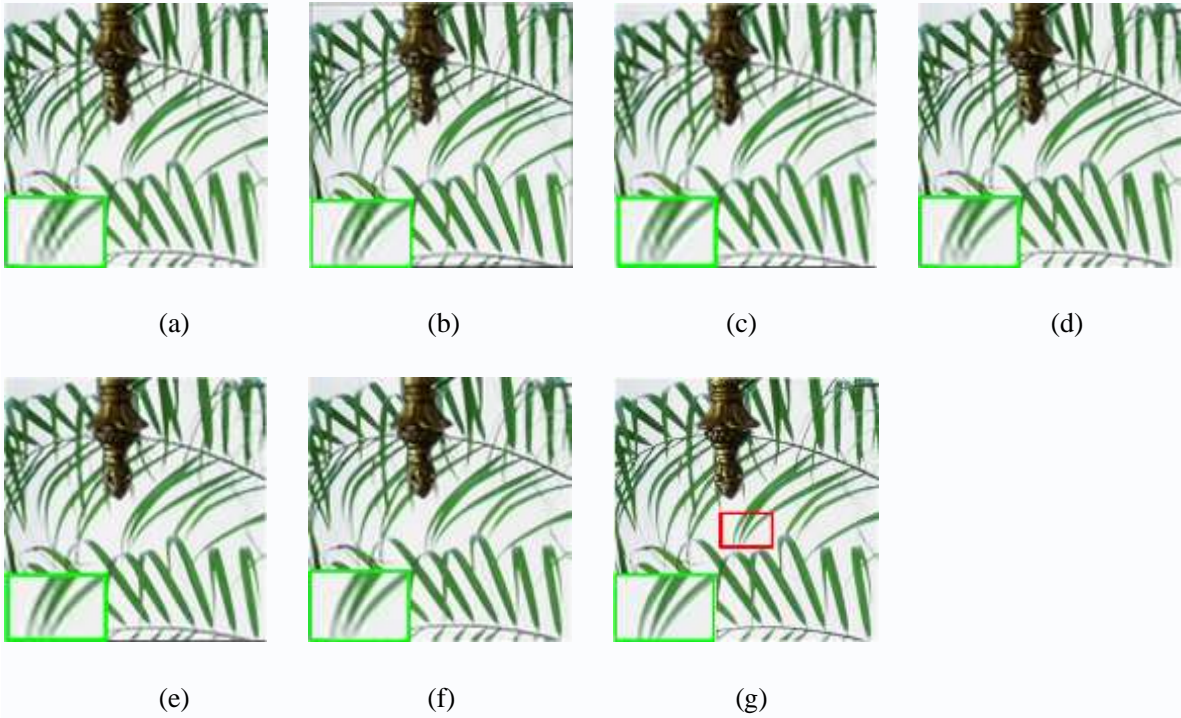


Fig.3 Super-resolved images ( $3\times$ ) of Leaves with different methods. The area in green rectangle is the  $2\times$  local magnification of red rectangle in each example. (a) Result of SC-based method. (b) Result of SPM. (c) Result of ANR. (d) Result of ASDS. (e) Result of AULF. (f) Result of proposed method. (g) The original HR image.

To assess the visual quality, we show  $3\times$  magnification results of Butterfly and Leaves in Figs 2 and 3 respectively. The ASDS method can preserve edges and suppress noise well. Our proposed method can produce less artifacts, sharper edges and more faithful detail. This performance can be readily observed in the resulting image “Leaves”, where the edges generated by our proposed method are clearer and sharper.

#### 4.4. Experiments on images with artificially added noise

In this subsection, we carry out SR experiments on noisy images to explore the extent to which our

proposed method is robust against noise. Because SPM and ANR are known to perform on images without artificially added noise [32, 44], we do not show comparative evaluation results for these two methods in our numerical results (table 5). The noisy LR images are generated from the original HR image by applying a  $7 \times 7$  Gaussian kernel of standard deviation 1.6, then decimating by a factor of 3, and then contaminating the resulting image by Gaussian white noise with standard deviation 5 [11]. Table 5 presents the objective evaluation results of PSNR and SSIM values. We can see that, under noisy conditions, the proposed method is superior to other SR algorithms in terms of the averaged results of PSNR and SSIM over all eight images. However, for two images out of eight, the proposed algorithm is slightly inferior to the results of AULF. This may be due to the fact that we use an ASDS-AReg based sparse representation that learns sub-dictionaries from external images to “hallucinate” details.

Table 5 PSNR (dB) and SSIM results of eight test images for  $3 \times$  magnification ( $\sigma_n = 5$ ).

Test image	SC [51]	SPM [32]	ANR [44]	ASDS [11]	AULF [54]	Proposed method
Butterfly	25.02	–	–	26.08	26.88	<b>27.02</b>
	0.840			0.861	0.859	<b>0.875</b>
Hat	29.75	–	–	29.70	<b>30.15</b>	29.96
	0.819			0.816	<b>0.821</b>	0.813
Leaves	24.52	–	–	25.50	26.05	<b>26.15</b>
	0.841			0.865	0.874	<b>0.883</b>
Plants	31.31	–	–	31.10	<b>31.61</b>	31.33
	0.854			0.836	<b>0.846</b>	0.838
Elephants	30.27	–	–	30.04	30.41	<b>30.49</b>
	0.755			0.747	0.749	<b>0.754</b>
Woman	29.65	–	–	29.77	30.27	<b>30.54</b>
	0.869			0.877	0.871	<b>0.878</b>
Red flower	29.77	–	–	29.49	29.62	<b>29.77</b>
	0.844			0.833	0.828	<b>0.836</b>
Building	24.73	–	–	24.70	25.57	<b>25.76</b>
	0.695			0.679	0.706	<b>0.716</b>
average	28.12	–	–	28.29	28.82	<b>28.87</b>
	0.814			0.814	0.819	<b>0.824</b>

#### 4.5. Discussion of computational cost

As illustrated in Tables 1 and 2, the proposed SR method incurs major costs in two main parts: the GA method and the regularization prior model. Let the super-resolved image size be  $nm$ . In the first stage, the computational cost is related to two factors: iteration times  $t_1$  and the population size  $N$ . The fitness values of the individuals cost approximately  $O(t_1Nm^2n^2)$  and the crossover and mutation cost approximately  $O(t_1mn)$ , so that the total cost of the first stage is approximately  $O(t_1(Nm^2n^2+mn))$ . In the second stage, the main costs are the computation of the NLM weight matrix and iteratively updating the HR image. The computation of the NLM weight matrix is related to three factors: the searching radius  $r$ , the size of local analysis window  $d$ , and the super-resolved image size  $nm$ . Hence, it takes overall  $O(mnd^2r^2)$  to evaluate the NLM weight matrix for all the pixels. The gradient decent is  $t_2$  iterations and the second stage cost is approximately  $O(t_2(Qq^2+4m^2n^2+6mn)+mnd^2r^2)$ .

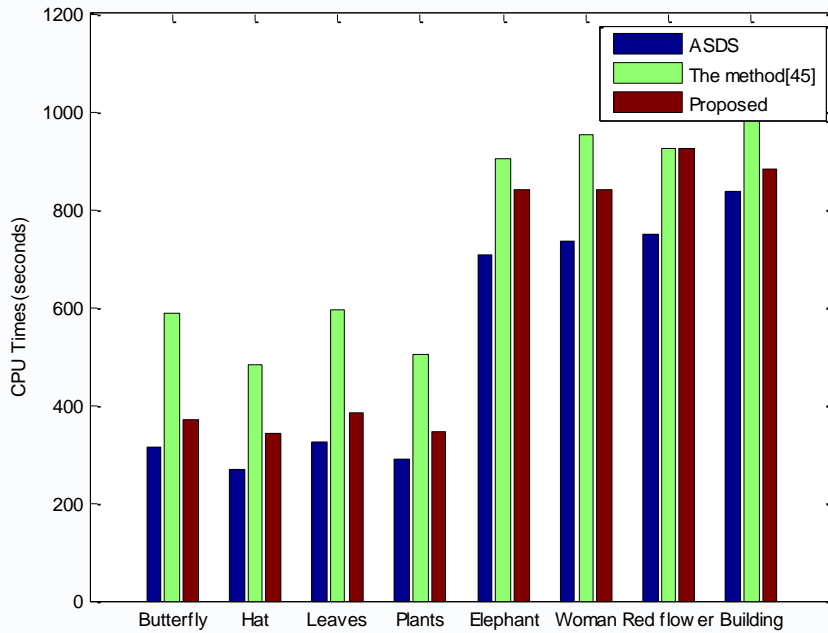


Fig.4. Comparisons of CPU time between the ASDS method, the AULF method and the proposed method.

#### 4.6. Discussion of computation time and the convergence rate

We have compared the proposed method with ASDS and AULF in terms of CPU time. Fig.4 shows the CPU time spent on all the test images, using MATLAB 7.10(R2010a) on a Windows Server with 2.00GB of RAM and two i3 Intel cores of 2.4-GHz. The proposed SR method costs less than AULF, and only slightly

more than ASDS, while still producing higher quality SR image recovery. Because the GA is combined with the ASDS-AReg, the iteration times in the second stage are reduced. From Fig.5, it can be seen that the proposed method converges more quickly compared with conventional ASDS. Moreover, the proposed method consistently performs better than ASDS.

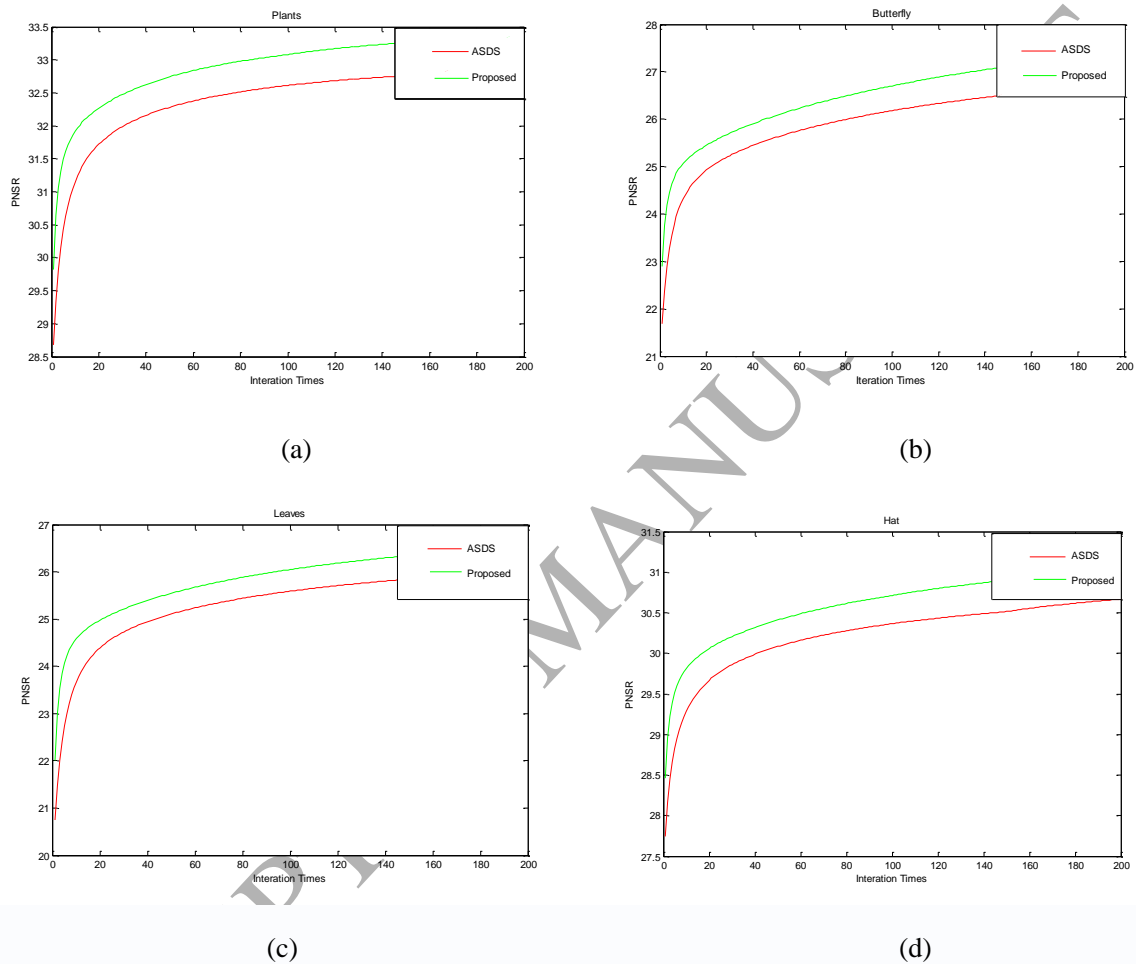


Fig.5. Comparisons of convergence rate between ASDS method and proposed method. (a) PNSR changes of Plants, (b) PNSR changes of Butterfly, (c) PNSR changes of Leaves, (d) PNSR changes of Hat.

## 5. Conclusion

In this paper, we approach single image SR reconstruction as an optimization problem, and propose a new single image SR framework which combines the GA and a regularization prior model. Firstly, for avoiding local minima, we use a GA to search the solution space and obtain an improved HR image. Secondly, we use a regularization prior model to perform a single-point search in the solution space, and

obtain higher quality SR estimation. Finally, empirical experiments on a number of images, both with and without added noise, drawn from two different public benchmark data sets, suggest that the proposed method performs competitively in comparison to other state-of-the-art methods. In future work, based on sparse representation, other effective priors, such as SKR and edge priors, could be introduced into the ASDS-AReg to improve the proposed method.

#### Acknowledgment

This work was supported by the National Natural Science Foundation of China (Nos. 61272279, 61272282, 61371201, and 61203303), the Program for New Century Excellent Talents in University (No. NCET-12-0920), the National Basic Research Program (973 Program) of China (No. 2013CB329402), the Program for Cheung Kong Scholars and Innovative Research Team in University (No. IRT\_15R53), and the Fund for Foreign Scholars in University Research and Teaching Programs (the 111 Project) (No. B07048).

## References

- [1] Baker, S. and Kanade, T.. Limits on super-resolution and how to break them, *IEEE Trans. Pattern Anal. Mach. Intell.*, 24(9)(2002),pp. 1167-1183.
- [2] Bertero, M., and Boccacci, P.. *Introduction to Inverse Problems in Imaging*. Bristol, U.K.: IOP, 1998.
- [3] Besag, J.. On the Statistical-Analysis of Dirty Pictures. *Journal of the Royal Statistical Society*, 1986, B-48(5-6):259-302.
- [4] Buades, A., Coll, B., and Morel, J. M.. A review of image denoising algorithms, with a new one, *Multiscale Model Simul.*, 4(2)(2005), pp.490-530.
- [5] Candocia, F. M., and Principe, J. C.. Super-resolution of images based on local correlations, *IEEE Trans. Neural Netw. Learn. Syst.*, 10(2)(1999), pp.372-380.
- [6] Chang, H., Yeung, D.-Y., and Xiong, Y.. Super-resolution through neighbor embedding, in *Proc. IEEE Conf. Computer Vision and Pattern Recognition*, pp.275-282, Jul, 2004.
- [7] Chuang, Y. C., Chen, C. T., and Hwang, C.. A real-coded genetic algorithm with a direction-based crossover operator. *Information Sciences*, 2015, 305:320-348.
- [8] Contreras-Bolton, C., and Parada, V.. Automatic Combination of Operators in a Genetic Algorithm to Solve the Traveling Salesman Problem. *Plos One*, 2015, 10(9).
- [9] Daubechies, I., Defriese, M., and De Mol, C.. An iterative thresholding algorithm for linear inverse problems with a sparsity constraint, *Commun. Pure Appl. Math.*, 57(2004), pp.1413-1457.
- [10] Dong, C., Loy, C. C., He, K., et al.. Image Super-Resolution Using Deep Convolutional Networks. *IEEE Transactions on Pattern Analysis & Machine Intelligence*, 2014, 38(2):1-1.
- [11] Dong, W., Zhang, L., Shi, G., and Wu, X.. Image deblurring and super-resolution by adaptive sparse

- domain selection and adaptive regularization, *IEEE Trans. Image Process.*, 20(7)(2011), pp.1838-1857.
- [12] Drake, J. H., Özcan, E., and Burke, E. K.. A Case Study of Controlling Crossover in a Selection Hyper-heuristic Framework using the Multidimensional Knapsack Problem. *Evolutionary Computation*, 2016, 24(1):113-141.
- [13] Elad, M. and Aharon, M.. Image denoising via sparse and redundant representations over learned dictionaries, *IEEE Trans. Image Process.*, 15(12)(2006), pp.3736-3745.
- [14] Farsiu, S., Robinson, M. D., Elad, M., and Milanfar, P.. Fast and robust multi-frame super resolution, *IEEE Trans. Image Process.*, 13(10) (2004), pp.1327-1344.
- [15] Freeman, W. T., Thouis, R. J., and Egon, C. P.. Example-based super-resolution, *IEEE Computer Graphics and Applications.*, 22(2)(2002), pp.56-65.
- [16] Gao, X., Lu, W., Tao, D., and Li, X.. Image quality assessment based on multiscale geometric analysis, *IEEE Trans. Image Process.*, 18(7)(2009), pp.1409-1423.
- [17] Geman, S., and Geman, D.. Stochastic Relaxation, Gibbs Distributions, and the Bayesian Restoration of Images. *IEEE Transactions on Pattern Analysis & Machine Intelligence*, 1984, 6(6):721-41.
- [18] Goldberg, D. E.. *Genetic Algorithms in Search, Optimization, and Machine Learning*, New York: Addison-Wesley, 1989.
- [19] Gong, W., Hu, L., Li, J., et al.. Combining sparse representation and local rank constraint for single image super resolution. *Information Sciences*, 2015, 325:1-19.
- [20] Holland, J.. *Adaptation in Natural and Artificial Systems*, University of Michigan Press, Ann Arbor, 1975.
- [21] Huang, T. S. and Tsai, R. Y.. Multi-frame image restoration and registration, *Adv. Comput. Vis. Image*

- Process., 1(2)(1984), pp.317-339.
- [22] Kindermann, S., Osher, S., and Jones, P. W.. Deblurring and denoising of images by nonlocal functionals, *Multiscale Model. Simul.*, 4(4)(2005), pp.1091-1115.
- [23] Li, J., Gong, W., Li, W.. Dual-sparsity regularized sparse representation for single image super-resolution. *Information Sciences*, 2015, 298(C):257-273.
- [24] Li, X. and Orchard, M. T.. New edge-directed interpolation, *IEEE Trans. Image Process.*, 10(10)(2001), pp.1521-1527.
- [25] Li, X., He, H., Wang, R., and Tao, D.. Single Image Super-resolution via Directional Group Sparsity and Directional Features., *IEEE Trans. Image Process.*, 24(9)(2015), pp.2874-2888.
- [26] Li, X., Hu, Y., Gao, X., Tao, D., and Ning, B.. A multi-frame image super-resolution method, *Signal Process.*, 90(2)(2010), pp.405-414.
- [27] Liu, J., Ding, Y., Zhou, P., and Liu, L.. Image super-resolution reconstruction based on parallel genetic algorithm, *Journal of Image and Graphics.*, 9(1)(2004), pp.62-68.
- [28] Mackenzie, M. and Tieu, A. K.. Asymmetric kernel regression, *IEEE Trans. Neural Netw.*, 15(2)(2004), pp.276-282.
- [29] Mairal, J., Bach, F., Ponce, J., Sapiro, G., and Zisserman, A.. Non-local sparse models for image restoration, in *Proc. IEEE Int. Conf. Comput. Vis.*, 2009, pp.2272-2279.
- [30] Marquina, A., and Osher, S. J.. Image super-resolution by TV regularization and Bregman iteration, *J. Sci. Comput.*, 37(3)(2008), pp.367-382.
- [31] Michalewicz, Z.. *Genetic Algorithms + Data Structures = Evolution Programs*, New York: SpringerVerlag, 1996.
- [32] Peleg, T., and Elad, M.. A Statistical Prediction Model Based on Sparse Representations for Single



- Image Super-Resolution, *IEEE Trans. Image Process.*, 23(6)(2014), pp.2569-2582.
- [33] Protter, M., Elad, M., Takeda, H., and Millanfar, P. Generalizing the non-local means to super-resolution reconstruction, *IEEE Trans. Image Process.*, 18(1)(2009), pp.36-51.
- [34] Purkait, P., Pal, N. R., and Chanda, B.. A Fuzzy-Rule-Based Approach for Single Frame Super Resolution, *IEEE Trans. Image Process.*, 23(5)(2014), pp.2277-2290.
- [35] Ramteke M., Ghune, N., Trivedi, V.. Simulated binary jumping gene: A step towards enhancing the performance of real-coded genetic algorithm. *Information Sciences*, 2015, 325:429-454.
- [36] Sigitani, T., Iiguni, Y., and Maeda, H.. Image interpolation for progressive transmission by using radial basis function networks, *IEEE Trans. Neural Netw. Learn. Syst.*, 10(2)(1999), pp.381-390.
- [37] Stark, H., and Oskoui, P. High-resolution image recovery from image-plane arrays, using convex Projection, *J. Opt. Soc. Amer.*, 6(11)(1989), pp.1715-1726.
- [38] Stolkin R., Greig, A., Hodgetts, M., et al.. An EM/E-MRF algorithm for adaptive model based tracking in extremely poor visibility. *Image & Vision Computing*, 2008, 26(4):480–495.
- [39] Stolkin, R., Hodgetts, M., Greig, A.. An EM / E-MRF Strategy for Underwater Navigation. *Bmvc*, 2000.
- [40] Stolkin, R., et al.. Extended Markov Random Fields for predictive image segmentation. *Proceedings of the 6th International Conference on Advances in Pattern Recognition*. 2007.
- [41] Sun, J., Zhang, Y., Garibaldi, J.M., et al.. A Multi-cycled Sequential Memetic Computing Approach for Constrained Optimisation. *Information Sciences*, 2016, 340-341:175-190.
- [42] Sun, J., Xu, X., and Shum, H.. Image super-resolution using gradient profile prior, in *Proc. IEEE Conf. Comput. Vis. Pattern Recog.*, 2008, pp.1-8.
- [43] Tai, Y., Liu, S., Brown, M. S., and Lin, S.. Super resolution using edge prior and single image detail

- synthesis, in Proc. IEEE Conf. Comput. Vis. Pattern Recognit., 2010, pp.2400-2407.
- [44] Timofte, R., De Smet, V., and Van Gool, L.. Anchored Neighborhood Regression for Fast Example-Based Super-Resolution., in Proc. IEEE Int. Conf. Comput. Vis., 2013, pp.1920-1927.
- [45] Wang, N., Tao, D., Gao, X., and Li, X.. Transductive Face Sketch-Photo Synthesis, IEEE Trans. Neural Netw. Learn. Syst., 24(9)(2013), pp.1364-1376.
- [46] Wang, N., Tao, D., Gao, X., Li, X., and Li, J.. A Comprehensive Survey to Face Hallucination, Int. J. Comput. Vis., 106(1)(2014), pp.9-30.
- [47] Wang, N., Li, J., Tao, D., Li, X., and Gao, X.. Heterogeneous image transformation, Pattern Recognition Letters, 34(4)(2013), pp.77-84.
- [48] Wang, Z., Bovik, A. C., Sheikh, H. R., and Simoncelli, E. P.. Image quality assessment: From error visibility to structural similarity, IEEE Trans. Image Process., 13(4)(2004), pp.600-612.
- [49] Wen, X. Z., Shao, L., Xue, Y., and Fang W.. A rapid learning algorithm for vehicle classification, Information Sciences, 295(1), pp. 395-406, 2015.
- [50] Wu, X., Zhang, X., and Wang, J.. Model-guided adaptive recovery of compressive sensing, in Proc. Data Compression Conference, pp.123-132, 2009.
- [51] Yang, J., Wright, J., Huang, T., and Ma, Y.. Image super-resolution via sparse representation, IEEE Trans. Image Process., 19(11)(2010), pp.2861-2873.
- [52] Yang, J., Wang, Z., Lin, Z., Cohen, S., and Huang, T.. Coupled Dictionary Training for Image Super-Resolution, IEEE Trans. Image Process., 21(8)(2012), pp.3467-3478.
- [53] Yu S., Kang, W., Ko, S., et al.. Single image super-resolution using locally adaptive multiple linear regression. Journal of the Optical Society of America A, 32(12) (2015), pp.2264-2275.
- [54] Yu, J., Gao, X.. A unified learning framework for single image Super-resolution, IEEE Trans. Neural Netw. Learn. Syst., 25(4)(2014), pp.780-792.

- [55] Zeyde, R., Elad, M., and Protter, M.. On Single Image Scale-Up Using Sparse-Representations, in Proc. 7 th Int. Conf. Curves Surf., 2010, pp.711-730.
- [56] Zhang, K., Gao, X., Tao, D., and Li, X.. Single Image Super-Resolution With Non-Local Means and Steering Kernel Regression, IEEE Trans. Image Process., 21(11)(2012), pp.4544-4556.
- [57] Zhang, K., Gao, X., Li, X., and Tao, D.. Partially supervised neighbor embedding for example-based image super-resolution, IEEE J. Sel. Topic Signal Process., 5(2)(2011), pp.230-239.
- [58] Zhang, L. and Wu, X.. An edge-guided image interpolation algorithm via directional filtering and data Fusion, IEEE Trans. Image Process., 15(8)(2006), pp.2226-2238.
- [59] Zhang, L., Lukac, R., Wu, X., and Zhang, D.. PCA-based spatially adaptive denoising of CFA images for single-sensor digital cameras, IEEE Trans. Image Process., 18(4)(2009), pp.797-812.
- [60] Zhang, L., Dong, W., Zhang, D., and Shi, G.. Two-stage image denoising by principal component analysis with local pixel grouping, Pattern Recognition, 43(2010), pp.1531-1549.



**Yangyang Li** received the B.S. and M.S. degrees in Computer Science and Technology from Xidian University, Xi'an, China, in 2001 and 2004 respectively, and the Ph.D. degree in Pattern Recognition and Intelligent System from Xidian University, Xi'an,

China, in 2007.

She is currently a professor in the school of Electronic Engineering at Xidian University. Her current research interests include quantum-inspired evolutionary computation, artificial immune systems, and data mining.